Chinese Journal of Physiology 52(5 Supplement): 384-394, 2009
DOI: 10.4077/CJP.2009.AMK033

Enhancement of Vascular Formation But Not Improvement of Ventricular Function of Infarcted Rat Hearts by a High Dose of Adenovirus-Carried VEGF Transgene

Ruey-Jen Sung[1], Shu-Hui Chen[2], Chwan-Yan Luo[3], Jieh-Neng Wang[4], Chao-Liang Wu[5], Yun-Hsiang Chen[6], Rey-Jyh Su[6], Huey-Jiun Li[6], and Mei-Ling Tsai[6]

[1]Departments of Internal Medicine, [2]Chemistry, [3]Surgery, [4]Pediatrics, [5]Biochemistry, [6]Physiology, National Cheng Kung University, Tainan, Taiwan, Republic of China

Abstract

The purpose of this study was to examine the influence of adenovirus-carried VEGF165 transgene at 5×10^{10} pfu (Ad-VEGF) on vascular formation, cardiac geometry and ventricular function in infarcted hearts of the rat and to explore the mechanism of Ad-VEGF-mediated actions on ventricular function by quantitative proteomic analysis. Seven days after coronary occlusion, intramyocardial injection with normal saline (vehicle control), adenovirus-carried beta-galactosidase gene (Ad-LacZ, vector control) or Ad-VEGF to infarcted hearts was conducted. Seven days after intramyocardial injection, ventricular function, cardiac morphology and vascular density were assessed after echocardiographic analysis and immunohistological staining. One dimensional gel electrophoresis coupled with stable isotope dimethyl labeling and LC/MS/MS was used to quantify the abundance ratio of each protein pair in Ad-VEGF- and Ad-LacZ-treated hearts. Our data indicated that both Ad-VEGF and Ad-LacZ increased arteriolar densities. However, the former increased arterial densities but the latter did not. Compared with the vehicle control, Ad-LacZ reversed occlusion-induced wall thinning and functional impairment but Ad-VEGF did not. Quantitative proteomic analysis showed increased ratios of plasma proteins (such as albumin) and oxygen carriers (such as myoglobin) by Ad-VEGF and decreased ratios of proteins involved in glycolysis, calcium homeostasis and lipolysis by Ad-VEGF. Taken together, our functional, morphological and proteomic data suggest that intramuscular delivery of Ad-LacZ at higher doses may improve ventricular function and wall thinning with arteriolar formation. Excessive amounts of VEGF by Ad-VEGF may offset Ad-LacZ-induced improvement in ventricular functions by interfering with calcium homeostasis and lipolysis in infarcted hearts.

Key Words: adenovirus, gene therapy, quantitative proteomics, infarction, VEGF, arteriogenesis, rat, ventricular function

Introduction

Despite substantial reduction in mortality over the past 30 years, ischemic heart diseases still remain the leading cause of death in developed countries (16). Several conventional therapies including percutaneous coronary interventions, indeed, improve ventricular functions with the induction of revascularization in the ischemic heart. However, the patients who are not suitable for conventional treatment are seeking alternative therapies such as therapeutic angiogenesis (18, 19).

Corresponding author: Dr. Mei-Ling Tsai, Department of Physiology, National Cheng Kung University Medical College, Tainan 70101, Taiwan, ROC. Tel: +886-6-2353535 ext. 5436, Fax: +886-6-2362780, E-mail: mltsai@mail.ncku.edu.tw
Received: April 28, 2009; Revised: August 14, 2009; Accepted: September 29, 2009.
 ISSN : 0304-4920. http://www.cps.org.tw

VEGF gene therapy, which induces new vessel formation, has been applied to treatment of ischemic cardiovascular diseases (13, 17). Some studies show improvement in ischemia-induced clinical signs after intramyocardial injection of VEGF transgene but some do not (5, 7, 27, 30). Even though VEGF transgene including both the plasmid encoding human VEGF gene (phVEGF, about 2,000 μg DNA/person) and adenovirus carried-VEGF transgene (Ad-VEGF, about 2×10^{10} pfu/person) may not improve ventricular function of patients with chronic myocardial ischemia, Ad-VEGF still improves myocardial perfusion and phVEGF does not (7). In rats, phVEGF (about 40 μg DNA/rat) induces the expression of VEGF to a lesser extent than Ad-VEGF (about 5×10^9 pfu/rat) but both elicit similar effects on functional improvement of infarcted hearts (6). It becomes clear that adenovirus provides a better delivery system than the plasmid alone.

The failure of Ad-VEGF transgenes in improving ventricular function of infarcted hearts may be, in part, due to insufficient amounts of Ad-VEGF that cannot augment myocardial perfusion to critical levels. However, VEGF transgene at the dose of 500 μg DNA/rat causes angioma formation in rats with chronic myocardial infarction (24). Ad-VEGF at 2×10^{10} pfu causes edema in ischemic skeletal muscles (29). Since no report has explored if Ad-VEGF at dosages greater than 2×10^{10} pfu can improve ventricular function of infarcted hearts, the first aim of this study was to examine the influence of Ad-VEGF at 5×10^{10} pfu on ventricular function of infarcted hearts. Additionally, the effects of Ad-VEGF on vascular densities and cardiac geometry in infarcted rat hearts were investigated.

Furthermore, possible mechanism of Ad-VEGF-mediated actions in infarcted hearts was explored. To date, proteomic analysis has been used to discover novel mechanisms in biomedical studies. Conventionally, two-dimensional gel electrophoresis (2D gel) coupled with LC/MS/MS has been widely used to reveal proteins on a large scale basis. Because of its limitation in separating proteins with extreme properties such as high hydrophobicity, one dimensional gel electrophoresis (1D gel) coupled with LC/MS/MS, termed as geLC/MS/MS, is developed to identify hydrophobic proteins. However, poor resolution of geLC/MS/MS has limited its application in quantifying the relative changes of those proteins (1, 23). Since the development of the technique of stable isotope dimethyl labeling coupled with LC/MS/MS, accuracy in quantifying the relative change of each protein identified has been dramatically improved (9, 10). Accordingly, our second aim was to explore the mechanism of Ad-VEGF-mediated actions in infarcted hearts by quantitative proteomic analysis using a combination of geLC/MS/MS and the technique of stable isotope dimethyl labeling. Discovery of VEGF-mediated shifts in the abundance ratio of various proteins may support our functional results and provide a molecular basis by which the mechanism of Ad-VEGF-mediated actions on ventricular function is proposed.

Materials and Methods

Animal Care

Male Wistar rats at the age of 8 weeks (weight 270-300 g) were housed in the colony at the Animal Center of the National Cheng Kung University Medical College. The temperature was kept at 24 ± 1°C under a 14-hr light (0500-1900) cycle. Operation procedures in our animal studies were based on the Guide for the Care and Use of Laboratory Animals published by the US National Institutes of Health (NIH Publication No. 85-23, revised 1996). All experimental protocols were approved by the National Cheng Kung University Animal Care and Use Committee, Taiwan.

Adenoviral Vector Construction

Replication-defective adenoviral vector based on E1/E3-deleted adenovirus type 5 was generated. The 573-bp fragment containing the coding region of the human VEGF165 gene from pBLAST49-hVEGF (Invivogen, San Diego, CA, USA) was cloned into the adenovirus shuttle vector pAd5L. The resulting plasmid was co-transfected with pJM17 into 293 cells to generate Ad-VEGF. Ad-LacZ was used a control vector.

Protocols of Animal Studies

After inhalation with isoflurane (1.5 ± 0.5%), anesthetized rats were intubated with an 18 gauge intravenous catheter and connected to a volume-controlled ventilator at a tidal volume of 2.5 ml and respiratory rate of 90 times/min. After thoracotomy in the fourth left intercostal space, the heart was rapidly exteriorized. A 6-0 silk suture was passed and tightened around the base of the left anterior descending coronary artery. After dark discoloration appeared on the anterior and lateral wall of the left ventricle, ribs were pulled together with 3-0 silk and muscle layers and skin were closed.

Seven days after surgery, ventricular function of each rat was assessed by echocardiography. All ligated rats were randomly and evenly assigned into one of three groups: Ad-VEGF, Ad-LacZ (vector control) and normal saline (NS, vehicle control). Additional rats were used as sham controls. Seven

or fourteen days after intramyocardial injections, the ventricular function of each rat was assessed by echocardiography. After functional assessment, the heart was then isolated, perfusion-fixed with 10% phosphate-buffered formalin (1:1 diluted in PBS) for 10 min and cut into three transverse slices 3 mm thick from the apex to the ligation site. After discarding the caudal slice, the cranial slice (adjacent to the ligation site) was kept for histological analysis and the middle slice was collected for immunoblotting analysis.

Analysis of Myocardial Function by Echocardiography

A SONOS 5500 imaging system (Agilent Technologies, Andover, MA, USA) and a 12-MHz transducer was used to collect echocardiographic images by a blinded investigator. Two-dimensionally targeted M-mode images of the left ventricle (LV) obtained along the short-axis view at the mid-papillary level were used to measure left ventricular posterior wall thickness at diastolic phase (LVPWd) and left ventricle internal diameter during diastole (LVIDd). Fractional shortening (FS) was measured based on the equation: (LV end diastolic dimension [LVEDD]-LV end systolic dimension [LVESD])/LVEDD × 100%. End-diastolic (EDV) and end-systolic (ESV) left ventricular volumes were obtained by the biplane area-length method. Left ventricular ejection fraction (EF) (%) was calculated as [(EDV-ESV) ÷ EDV] × 100%.

Preparation of Tissue Homogenates

Cardiac tissues were minced and ground in the lysis buffer the composition of which is listed as follows: 20 mM Tris (hydroxymethyl) methylamine (BDH, London, England), 150 mM NaCl (Merck, Darmstadt, WI, USA), 1 mM Ethylenediaminetetraacetic acid, 1% (v/v) Nonidet P40 (BDH). After centrifugation at 7,500 g, 4°C for 20 min by a microcentrifuge (Microfuge R, Beckman, Fullerton, CA, USA), protein content in the supernatant was measured by the method of Lowry assay. Bovine serum albumin was used as the standard.

Immunoblot Analysis of VEGF Protein

Tissue homogenates (100 μg protein/lane) were loaded to each lane in a 12% SDS polyacrylamide gel. The positive control from HUVEC was added in a different lane. The proteins in the gel were transferred onto a polyvinyldifluoride membrane (NEN, Boston, MA, USA). The membrane was then treated with primary antibodies against VEGF (Transduction Lab., Lambertville, KY, USA) and a secondary antibody (goat anti-mouse IgG, Santa Cruz Biotechnology, Santa Cruz, CA, USA) labeled with peroxidase. According to the manufacturer protocol (ECL, NEN, Boston, MA, USA), chemiluminescence reagent was added to the treated membrane for band visualization. A background control was obtained when the primary antibodies were not added. The images were analyzed by a computerized image analyzer (UVP, Upland, CA, USA).

Immunohistochemistry

Sequential 3-5 μm sections were pretreated with 3% hydrogen peroxide with 10% serum to block nonspecific binding. After incubation with the primary antibody, anti-α-smooth muscle actin (α-SM actin) antibody (1:800, Santa Cruz) and anti-VEGF antibody (1:800, Santa Cruz) were used. The sections were then treated with the secondary antibody. Thirty min after adding an ABC reagent (Vector, Olean, CA, USA), peroxidase activity was detected using diaminobenzidine.

Quantitative Analysis of the Vascular Density

Morphometric analysis was carried out with a computerized imaging system (Amira 3.1, TGS, San Diego, CA, USA). The α-SM actin-positive vessels were further categorized by their structure. Vessels surrounded by α-SM actin-positive staining with no clear adventitia and the diameter less than 100 μm were defined as arterioles. The α-SM actin-positive vessels surrounded by adventitia and its diameter greater than 100 μm were defined as arteries. The density of arterioles and arteries for each animal was reported as a mean number of each size of vessels/mm^2 under lower and high power field. To minimize measurement errors, averages of the vessel numbers in the border zone were obtained from three different fields.

In-gel Protein Digestion

A 200 μg tissue homogenate from five hearts in the same group was pooled. A total protein amount of 200 μg from the pooled proteins was kept in the lysis buffer and loaded to each lane of a 8% SDS polyacrylamide gel (8 × 8 cm). The condition was the same as the standard protocol. After Brilliant Blue G-Colloidal Concentrate (Sigma-Aldrich, Saint Louis, MO, USA), 14 protein bands ranging from 200 to 30 kDa in the gels were cut out, washed twice with 50 mM NH_4HCO_3/50% ACN (1:1) for 15 min, and dehydrated with 100% ACN. Cysteins were reduced with 10 mM DTT in 100 mM NH_4HCO_3 for 45 min at 56°C followed by alkylation with 55 mM iodoacetamide in

100 mM NH_4HCO_3 for 30 min at room temperature and in the dark. The mixture from each band was washed again with 50 mM NH_4HCO_3 to remove excess reagents and dehydrated with 100% ACN for 10 min. A volume of 10-20 ml of a 12.5 mg/ml trypsin solution (Promega-Catalys, Wallisellen, Switzerland) in 50 mM NH_4HCO_3 was added onto each band mixture. After incubation at 37°C overnight, peptides were extracted with 100 µl of 5% trifluoroacetic acid.

Dimethyl Labeling

After in-gel digestion, the peptide extract from each band was dried and redissolved with 200 µl of sodium acetate buffer (100 mM, pH 5-6). Formaldehyde-H_2 (4% in water, 10 µl) was added to the extract from the Ad-LacZ group and the extract from the Ad-VEGF group was labeled with formaldehyde-D_2. After addition of freshly prepared sodium cyanoborohydride (600 mM, 10 µl) to each mixture, the two mixtures were combined and redissolved in 5% acetonitrile/0.1% formic acid for later MS analysis.

Sodium cyanoborohydride was purchased from Sigma (St. Louis, MO, USA); sodium acetate was obtained from Riedel–de Haën (Seelze, Germany). Formaldehyde-H_2 (37% solution in H_2O) was purchased from J. T. Baker (Phillipsburg, NJ, USA). Formaldehyde-D_2 was obtained from Aldrich (Milwaukee, WI, USA). Water was deionized to 18 MΩ using a Barnstead NANO ultrapure water system.

Mass Spectrometry and Protein Identification

The ESI-MS/MS data were collected from a Q-TOF micro instrument (Micromass, Manchester, UK) equipped with a nanoflow HPLC system (LC Packings, Amsterdam, Netherlands). A volume of 10 µl of sample fraction was injected, concentrated by a C18 nano-precolumn cartridge (i.d. 300 µm × 1-mm, 5 µm C18, P/N160458, LC Packings) and then separated by a C18 column (i.d. 75 µm, o.d. 280 µm × 15-cm, 3 µm C18, LC Packings). Mobile phase A consisted of 0.1% formic acid in 5% acetonitrile solution and mobile phase B consisted of 0.1% formic acid in 95% acetonitrile solution; a linear gradient from 5% to 60% B over a 50-min period at a flow rate of 350 nL/min was applied. The outlet of the column was connected to an ESI tip using a capillary tubing (i.d. 20 µm, o.d. 280 µm).

For identification, MS/MS spectra generated peak list based on MassLynx 4.0 Global ProteinLynx. All sequential scans with the same precursor were combined. The survey scan was from m/z 400 to 1,600 and MSMS scan was from m/z 50 to 2,000. The threshold to switch from MS to MSMS was 10 counts and the switch from MSMS back to MS was set up for signals that fell below 3 counts or after 8 seconds. A QA score of 10 was used to filter MSMS with poor quality and the settings to generate the pkl-files were: background subtraction using a polynomial order of 15 and 20% peak curve; peak smoothing using Savitzky Golay mode with 3.00 channels and 2 smooths; peak centroid using a minimum of 4 peak widths at half height and 80% centroid top. NCBInr (rattus 35302 sequences) on MASCOT (http://www.matrixscience.com) was used for database search. The mass tolerance was set at 0.2 Da for both precursor and product ions. Carbamidomethyl and dimethyl labeling were chosen for fixed modifications and one trypsin miss cleavage was allowed. A peptide score with a P value < 0.05 and "rank1" (Best match for each MSMS) peptides were included. Only proteins with a $P < 0.05$ were regarded as identified proteins.

Quantitative Analysis of Dimethyl Labeled Peptides

For each protein, all dimethyl-labeled peptides were quantified by comparing the intensity ratios of isotopic peptide pairs (*D/H*) deduced from LC/MS and LC/MS/MS. For each protein, the density of each peptide from the Ad-VEGF group was divided by that of the same peptide from the Ad-LacZ groups. The ratios of all peptide pairs were expressed as means ± standard deviation (SD) which reflected the abundance ratio of that protein between Ad-VEGF- and Ad-LacZ-hearts. All proteins quantified were listed in Table 2. The ratio of Heat shock 70-kD protein 5 between Ad-VEGF and Ad-LacZ group was close to 1 which was used as our housekeeping control. Their differences in the ratio between Heat shock 70-kD protein 5 and the protein quantified with the P value less than 0.05 was considered significant changes.

Statistical Analysis

All data were expressed as means ± SE (standard error) except for the data derived from quantitative proteomic analysis. The influence of coronary ligation on cardiac function was analyzed by paired Student's t test. The data from the rest of the studies underwent one-way ANOVA (SYSTAT 10.2, SPSS Science, San Francisco, CA, USA). A P-value < 0.05 was considered statistically significant.

Results

Effect of Coronary Occlusion on Left Ventricular Function and Cardiac Morphology

On the 7th day post-occlusion, the ligated rats

Table 1. Echocardiographic data of infarcted hearts on the 7th day post-occlusion

Functional parameters	Sham	Ligated
Heart rate (beats/min)	242 ± 20	285 ± 35
Fractional shortening (%)	44 ± 6	28 ± 5*
Ejection fraction (%)	0.795 ± 0.071	0.221 ± 0.10*
Morphological parameters		
Left ventricular posterior wall thickness at end-diastolic phase	0.168 ± 0.015	0.189 ± 0.017
Left ventricle internal diameter at end-diastole	0.697 ± 0.041	0.832 ± 0.071

Asterisk (*) indicates a significant difference between the sham and the ligated groups ($P < 0.05$).

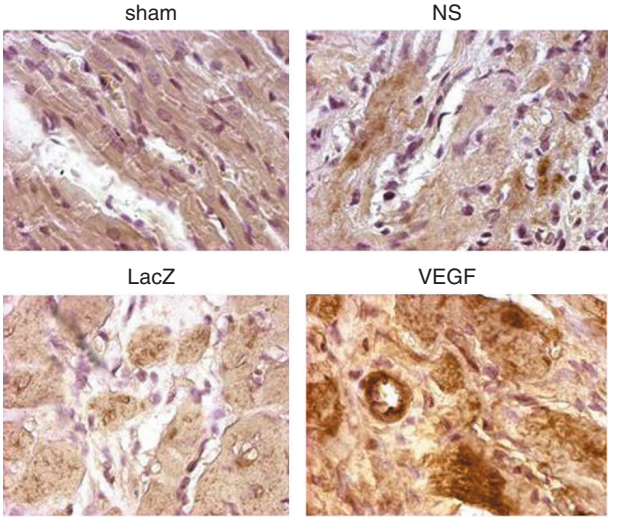

Fig. 1. Immunostaining for VEGF in rat hearts 7 days after intramyocardial injections. Dark brown: VEGF-positive staining. Only the ligated rats received the treatment of normal saline (NS, vehicle control), Ad-LacZ (LacZ, vector control) or Ad-VEGF (VEGF).

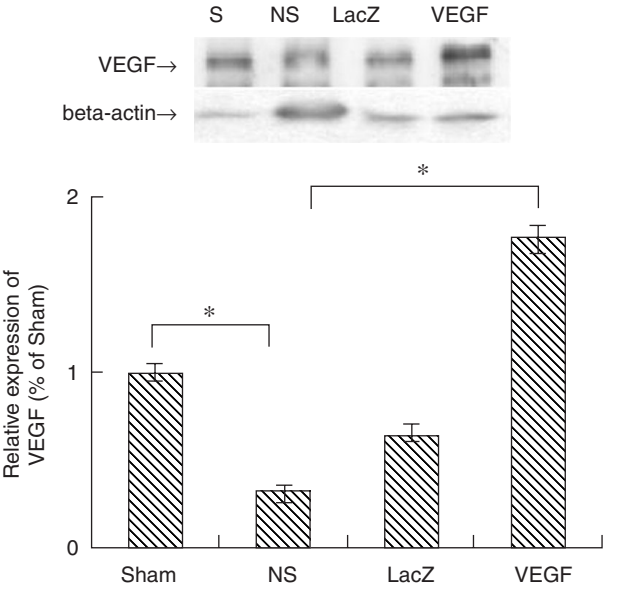

Fig. 2. Seven days after intramyocardial injections with Ad-VEGF (VEGF), Ad-LacZ (LacZ), or normal saline (NS), the abundance of VEGF in rat hearts was determined by immunoblotting. A representative blot is shown in the upper panel. After densitometry analysis, quantitative results of five separated experiments were summarized and expressed as means ± SE (lower panel). Asterisk (*) indicates statistical significance between the two groups.

had lower fractional shortening and ejection fraction without significant alterations in heart rate, the internal diameter of the left ventricle during diastole (LVIDd) and left ventricular posterior wall thickness at diastolic phase (LVPWd) (Table 1). Histological examination showing scar formation and wall thinning in the anteriolateral wall of the ligated hearts (data not shown) confirmed that the infarcted hearts wre in the subacute phase.

Protein Expression of VEGF and the Densities of Arterioles and Arteries in the Infarcted Hearts

Seven days after intramyocardial injection of Ad-VEGF to infarcted hearts, the expression of VEGF was confirmed by immunohistological studies and quantified by Western blotting. Ad-VEGF enhanced the intensity of positive staining for VEGF in the border zone of the infarcted hearts (Fig. 1) and the abundance of VEGF in the infarcted hearts (Fig. 2) but other treatments did not. Coronary occlusion did not affect arteriolar densities but lowered arterial densities in the border zone. Both Ad-LacZ and Ad-VEGF increased arteriolar densities ($P < 0.05$, Fig. 3); the former did not reverse the decrease of arterial densities by occlusion and the latter did (Fig 3).

Effect of Ad-VEGF on Cardiac Geometry and Ventricular Function

Seven days after injections, both Ad-LacZ and Ad-VEGF did not affect occlusion-induced decreases in fraction shortening. However, Ad-LacZ reversed occlusion-induced decreases in wall thickness and Ad-VEGF did not (Fig. 4). Fourteen days after injec-

Table 2. Functional annotation after quantitative analysis of identified proteins from infarcted rat hearts

Band	Accession number	Protein name	Mr. (Da)	matched peptides	Mean Ratio ± SD (Ad-VEGF/Ad-LacZ)
		Calcium homeostasis			
5	57303	sarcoplasmic reticulum Ca^{2+}-ATPase	111118	1	0.35
9	988307	calsequestrin	47896	4	0.47 ± 0.09*
9	62655719	similar to sarcalumenin	54805	2	0.54 ± 0.05*
		O_2 Carriers			
7	16758014	hemopexin	52012	4	0.72 ± 0.16
14	11024650	myoglobin	17204	4	0.21 ± 0.05*
14	204570	major beta-hemoglobin	16099	4	0.41 ± 0.13*
		Kreb's Cycle			
5	38541404	Aconitase 2, mitochondrial	86134	6	0.58 ± 0.15*
5	10637996	mitochondrial aconitase	86175	2	0.78 ± 0.18
9	220659	dihydrolipoamide succinyltransferase	47673	2	1.38 ± 0.03*
9	38303871	Dihydrolipoamide dehydrogenase (E3 component of pyruvate dehydrogenase complex)	54584	2	1.16 ± 0.09
12	18543177	citrate synthase	52182	2	0.90 ± 0.18
14	15100179	malate dehydrogenase 1, NAD	36634	2	0.76 ± 0.23
		ATP production			
9	203055	ATP synthase alpha subunit precursor	58906	6	0.43 ± 0.09*
9	1374715	ATP synthase beta subunit	51171	6	0.47 ± 0.07*
13	6671762	creatine kinase, muscle	43250	3	0.79 ± 0.21
13	62642723	similar to Creatine kinase, mitochondrial 2	38701	8	0.42 ± 0.09*
13	203480	creatine kinase	33426	6	0.47 ± 0.14*
		Cardiac Protection			
1	50657404	murinoglobulin 2	162879	13	1.23 ± 0.21
4	8393296	eukaryotic translation elongation factor 2	96209	2	0.68 ± 0.13
6	6175089	Serotransferrin precursor (Transferrin)	78577	10	0.82 ± 0.15
6	38303969	Heat shock 70kD protein 5	72476	4	1.09 ± 0.13
9	112889	Alpha-1-antiproteinase precursor	46281	5	0.79 ± 0.13
9	13928716	serine protease inhibitor 2c	45642	2	1.05 ± 0.13
		Lipolysis			
9	16073616	aldehyde dehydrogenase	48646	4	0.61 ± 0.08*
9	38541337	Acetyl-Coenzyme A dehydrogenase, long-chain	48248	4	0.47 ± 0.14*
11	2832739	mitochondrial very-long-chain acyl-CoA thioesterase	49960	2	0.72 ± 0.31
14	203900	delta-3,delta-2-enoyl-CoA isomerase	32191	3	0.51 ± 0.13*
		Glycolysis			
9	38303865	Glucose phosphate isomerase	62961	2	0.59 ± 0.13
11	6978809	enolase 1, alpha	47434	5	0.49 ± 0.21*
13	202837	aldolase A	39699	2	0.61 ± 0.04
13	56188	glyceraldehyde-phosphate-dehydrogenase	36103	2	0.31 ± 0.18*
14	62653460	similar to L-lactate dehydrogenase A chain (LDH-A)	36779	2	0.32 ± 0.16*
14	37590241	Lactate dehydrogenase B	36879	3	0.51 ± 0.04*
		Plasma Proteins			
8	55391508	Albumin	70744	13	1.43 ± 0.08*
9	121041	Ig gamma-1 chain C region	36503	1	1.64
		Others			
1	62642974	similar to hypothetical protein FLJ40243	253095	3	0.49 ± 0.11*
11	62079055	hypothetical protein LOC361596	51399	3	0.43 ± 0.21*
12	91997	aspartate transaminase, cytosolic	46631	5	0.32 ± 0.06*
14	56643	unnamed protein product	36097	12	0.89 ± 0.23

Asterisk (*) indicates a significant change when compared with the abundance ratio of heat shock 70-kDa protein 5 between Ad-VEGF- and Ad-LacZ-treated groups.

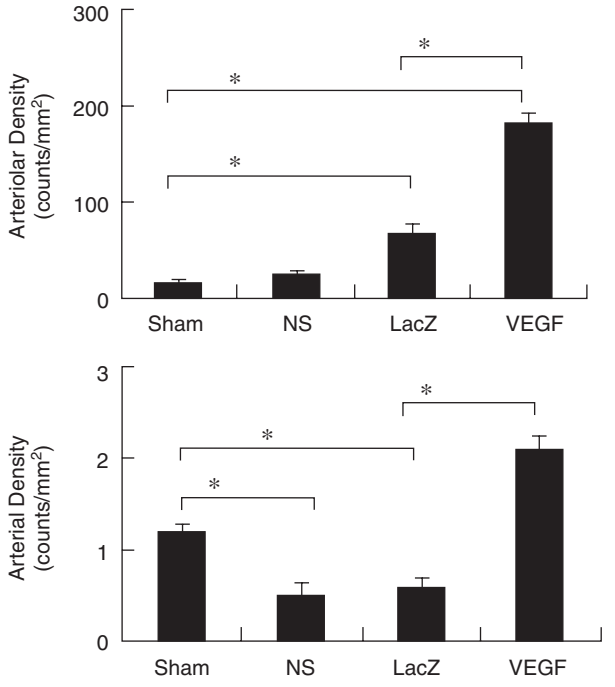

Fig. 3. The effect of Ad-VEGF on the density of α-SM actin-positive vessels in the border zone of infarcted hearts. The diameter of each vessel less than 100 μm was considered as an arteriole and that greater than 100 μm was considered as an artery. Quantitative data of arteriolar densities in the sham control (Sham) and the ligated groups treated with normal saline (NS), Ad-LacZ (LacZ) or Ad-VEGF (VEGF) are summarized in A and that of arterial densities are in B. Quantitative results of each group were expressed as means ± SE (lower panel). Asterisk (*) indicates statistical significance between the two groups.

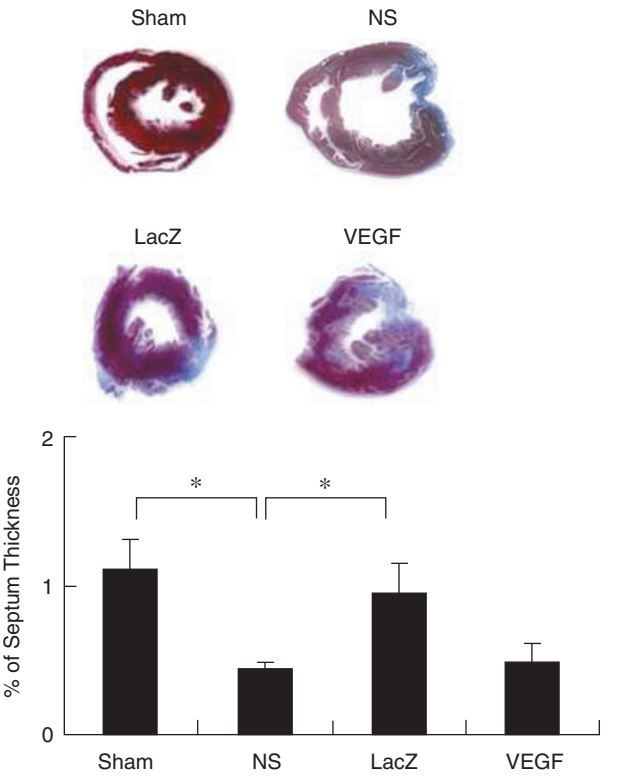

Fig. 4. Seven days after intramyocardial injections with Ad-VEGF (VEGF), Ad-LacZ (LacZ) and normal saline (NS), the wall thickness at the infarct area was measured after Trichrome staining. Light blue: accumulated collagens where scar tissues were formed. The heart in the Ad-VEGF group had greater blue areas than that in the Ad-LacZ (upper panel). Under a computerized imaging system, wall thickness was measured. Quantitative results of each group were expressed as means ± SE (lower panel). Asterisk (*) indicates statistical significance between the two groups.

tions, Ad-LacZ reversed occlusion-induced decreases in fraction shortening but Ad-VEGF did not (Fig. 5).

Influence of Ad-VEGF on the Profiling of Cardiac Proteins in Coomassie Blue-Stained Gel

To visualize Ad-VEGF-mediated shifts in the abundance of various proteins, 1D gel coupled with coomassie blue staining was conducted. Protein homogenates from four groups (sham control, ligated heart treated with normal saline, Ad-LacZ, and Ad-VEGF) were loaded into a 8% SDS gel and separated into 14 major bands. The strongest staining intensity in each group appeared at Band 8; the weakest staining intensity appeared at Bands 2, 3 and 4. When compared with the sham control, the ligated heart in the vehicle control group exhibited a lower intensity at Bands 8. Ad-LacZ reversed the occlusion-induced decrease in the staining intensity of Band 8 and Ad-VEGF further enhanced the decrease at Band 8 (Fig. 6).

To reveal the influence of Ad-VEGF on the shift in the abundance ratio of all proteins in each band, the technique of stable isotope dimethyl labeling coupled with geLC/MS/MS was used. The amounts of proteins in Bands 2, 3 and 4 which showed the weakest intensities were too low to calculate their ratios. Those at other bands were sufficient enough for quantification. Relative to Ad-LacZ, Ad-VEGF insignificantly increased the ratio of some proteins including murinoglobulin 2 in Band 1 to 1.23, Heat shock 70-kD protein 5 at Band 6 to 1.09, and Ig gamma-1 chain C region at Band 9 to 1.64, Dihydrolipoamide dehydrogenase at Band 9 to 1.09, and serine protease inhibitor 2c at Band 9 to 1.05 ($P > 0.05$).

Functional Annotation of Cardiac Proteins in Infarcted Hearts after Quantitative Proteomic Analysis

Functional annotation showed the increased

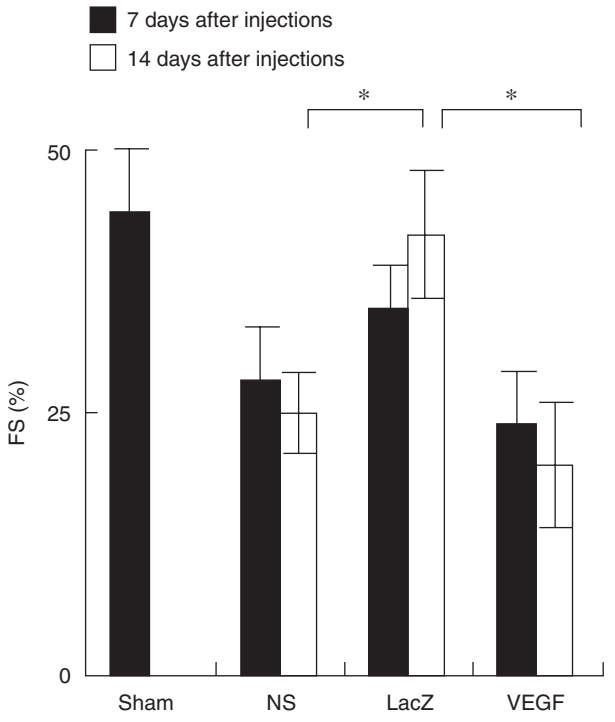

Fig. 5. Evaluation of ventricular functions by echocardiograph on the 7th (■) and 14th (□) day after intramyocardial injections. Five rats were used in each group. After echocardiographic measurement, fractional shortening (FS), as indication of ventricular contraction, was calculated and expressed as means ± SE for each group. Asterisk (*) indicates statistical significance between the two groups. NS: normal saline groups; LacZ: Ad-LacZ group; VEGF: Ad-VEGF group.

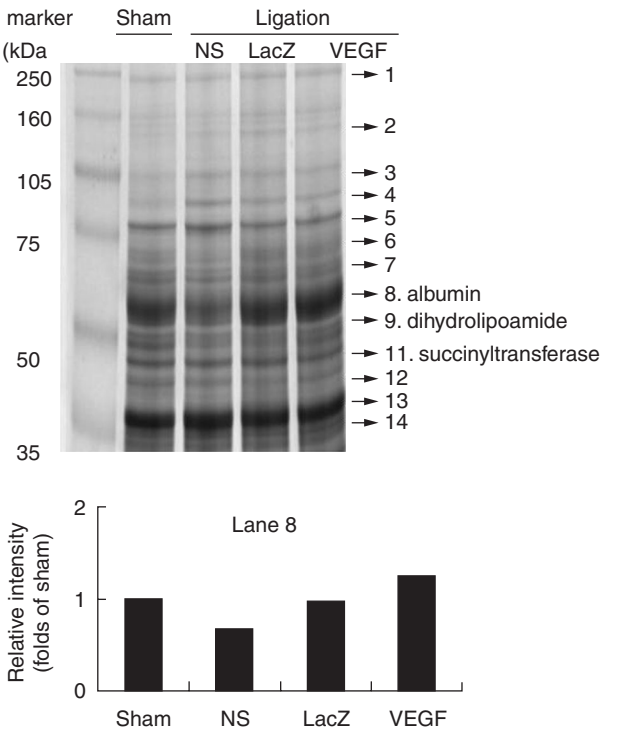

Fig. 6. One-dimensional gel from hearts from sham operation (Sham) or infarcted hearts treated with normal saline (NS), Ad-LacZ (LacZ) or Ad-VEGF (VEGF) (upper panel). The intensity of Band 8 in the 1-D gel was measured by densitometry. After normalization with the total density in Band 8 in the sham control, the relative intensities at Band 8 in other groups were expressed as folds of the control (lower panel).

ratios of plasma proteins (such as albumin and immunoglobulin gamma) by Ad-VEGF and the decreased ratio of enzymes involved in glycolysis and lipolysis (such as lactate dehydrogenase, acyl-coenzyme A dehydrogenase, and acetyl-coenzyme A dehydrogenase) by Ad-VEGF. Even the ratio of the proteins involved in ATP production, calcium homeostasis and oxygen transport was also reduced by Ad-VEGF.

Discussion

Although geLC/MS/MS has been used to identify mitochondrial proteins from normal human heart (28), limitations in separation resolution of 1D gel have restricted its application in differential proteomic analysis. This may explain why two-dimensional gel electrophoresis coupled with MALDI-MS has been widely used in differential proteomic analysis by which ventricular proteins associated with cardiac diseases were discovered (11, 12). Although the combination of 2D gel with density analysis discovers various proteins related to cardiac diseases, the analysis cannot reflect the relative changes of two or more proteins in one spot. With the development of stable isotope labeling which improves the accuracy of proteomic study, application of geLC/MS/MS to quantitative proteomic analysis has become feasible. This is the first report to demonstrate the feasibility of combining these technologies.

If Ad-VEGF at 5×10^{10} pfu used in our study indeed increases myocardial perfusion, VEGF, vascular densities, plasma proteins (such as albumin and immunoglobulin gamma) accumulated in infarcted hearts should be increased. Occlusion-induced hypoxia should be ameliorated; the relative abundance of hypoxia-induced glycolytic enzymes (3, 21) and oxygen binding proteins (such as myoglobin) (8, 20) should be reversed. As our data indicated, Ad-VEGF induced increases in the expression of VEGF and the densities of vessels. Both our gel image analysis and proteomic results showed an increased ratio of albumin in Band 8. The ratios of hypoxia-increased proteins (such as L-lactate dehydrogenase and myoglobin) were decreased by Ad-VEGF. Although coronary blood flow was not measured in this study, both vascular densities and proteomic analysis support

previous reports that VEGF-mediated gene therapy improves myocardial perfusion of ischemic hearts (5-7, 24, 27, 30).

In this study, the enhancement of both arterial and arteriolar formation by Ad-VEGF at 5×10^{10} pfu did not effectively improve ventricular function and wall thinning of infarcted rat hearts. In patients with chronic myocardial ischemia, delivery of Ad-VEGF (2×10^{10} pfu) causes inflammation with the increase of inflammation-related proteins in the plasma without further improvement in ventricular functions (7). Our results support the notion of Hedman *et al.* (7) that Ad-VEGF at dosages greater than 2×10^{10} pfu may not effectively improve ventricular functions even with Ad-VEGF-mediated increases in myocardial perfusion due, in part, to the induction of systemic inflammation.

In the report of Hedman *et al.* (7), Ad-VEGF (2×10^{10} pfu) treatment was associated with the increase of interleukin-6, a proinflammatory cytokine, but treatment with Ad-LacZ (2×10^{10} pfu) alone on inflammatory cytokines was not examined. It has been reported that adenovirus at dosages greater than 10^{10} pfu triggers gene expression of proinflammatory cytokines (31) and that at 2.5×10^{11} pfu facilitates leukocyte infiltration (14). In the hind-limb ischemia model, both Ad-LacZ and Ad-VEGF at 2×10^{10} pfu increases vessel densities in ischemic hind-limbs. However, the former does not induce greater amounts of VEGF in serum, hind-limb edema or myonecrosis but the latter does (29). Since our findings show improvement of occlusion-induced wall thinning by Ad-LacZ, but not by Ad-VEGF, both the reports of Vajanto *et al.* (29) and our findings suggest that Ad-LacZ at dosages greater than 10^{10} pfu can induce vessel formation. It is likely that Ad-VEGF at doses higher than 10^{10} pfu may exaggerate Ad-LacZ-induced inflammation and further induces arterial formation. Subsequently, the increased formation of arterioles by Ad-LacZ-induced inflammation may improve ventricular function and wall thickness of infarcted hearts. Ad-VEGF may exaggerate Ad-LacZ-induced inflammation and offset Ad-LacZ-mediated actions. Since no inflammation-related marker proteins have been identified and quantified in the protein list of our proteomic results, the speculation requires further investigation.

Our quantitative proteomic analysis shows that the decreased ratios of proteins were related to lipolysis and calcium hemostasis by Ad-VEGF. A large-scale analysis of gene expression has shown a positive association between lipolytic enzymes and ventricular function in infarcted hearts (26). Comparative proteomics has shown reduced abundance of lipolytic enzymes (such as enoyl-CoA hydratase or fatty acid binding protein) in infarcted or failing hearts (1, 12). Even enzymatic analysis shows a positive association between reduced activities of lipolytic enzymes and functional deterioration of failing hearts (25). Accordingly, our result that Ad-VEGF decreased the ratios of lipolytic enzymes suggests that the failure of Ad-VEGF at higher doses in the improvement of ventricular function may be, in part, due to the decrease of lipolytic enzymes by Ad-VEGF.

The sarcoplasmic reticulum (SR) plays an important role in regulating Ca^{2+}-movements. Reduction in the expression of SR proteins (such as SR Ca^{2+}-ATPase, Ca^{2+}-channels, calsequestrin, phospholamban and other regulatory proteins) is associated with the development of various heart diseases (4). Occurrence of dystrophic cardiac muscles is associated with the reduction in the abundance of the major Ca^{2+}-reservoir protein calsequestrin and sarcalumenin in SR (15). Taken together with the current studies, the result that Ad-VEGF reduced the ratios of Ca^{2+}-ATPase, calsequestrin and sarcalumenin by Ad-VEGF also suggests the reduction of ventricular function by Ad-VEGF. The result again supports our functional data that Ad-VEGF offsets the improvement of ventricular function by Ad-LacZ.

If Ad-VEGF counteracts Ad-LacZ-mediated improvement in ventricular function and wall thinning, in part, due to the excessive production of VEGF which exaggerates adenovirus-induced inflammation, it is of importance to review current studies of VEGF on inflammation. To date, VEGF receptors (VEGFR1 and VEGFR2) can be found in macrophages. Binding of VEGF to VEGFR1 enhances monocyte migration and facilitates neutrophile recruitment (2, 32). In the presence of local inflammation, over-expression of Ad-VEGF may exaggerate the progression of inflammatory bowel diseases (22). Current studies of VEGF on leukocyte activation support our speculation that Ad-LacZ at 5×10^{10} pfu may cause mild inflammation and then lead to arteriolar formation and functional improvement. Excessive production of VEGF by Ad-VEGF may exaggerate adenovirus-induced inflammation and offset Ad-LacZ-induced improvement.

In conclusion, quantitative proteomic analyses provide a set of biochemical data to support our functional data. Combination of functional assays, morphological measurement and a large-scale analysis of ventricular proteins allows us to speculate that excessive expression of VEGF by the high-dose of Ad-VEGF enhances vessel formation and reverses occlusion-induced hypoxia, but exaggerates Ad-LacZ-induced protective effects, in part, by accelerating adenovirus-induced inflammation. The speculated mechanism by which Ad-VEGF (at 5×10^{10} pfu)-induced inflammation down-regulates proteins related to calcium homeostasis and lipolysis requires further

investigation.

Acknowledgments

This work was supported by grants from the NSC93-2320-B-006-041 to RJ Sung and the NSC93-2320-B-006-041 to ML Tsai. The authors thank CW Lin, MC Fang and HH Yu for technical support.

References

1. Banfi, C., Brioschi, M., Wait, R., Begum, S., Gianazza, E., Fratto, P., Polvani, G., Vitali, E., Parolari, A., Mussoni, L. and Tremoli, E. Proteomic analysis of membrane microdomains derived from both failing and non-failing human hearts. *Proteomics* 6: 1976-1988, 2006.
2. Barleon, B., Sozzani, S., Zhou, D., Weich, H.A., Mantovani, A. and Marme, D. Migration of human monocytes in response to vascular endothelial growth factor (VEGF) is mediated *via* the VEGF receptor flt-1. *Blood* 87: 3336-3343, 1996.
3. Chavez, A., Miranda, L.F., Pichiule, P. and Chavez, J.C. Mitochondria and hypoxia-induced gene expression mediated by hypoxia-inducible factors. *Ann. N. Y. Acad. Sci.* 1147: 312-320, 2008.
4. Dhalla, N.S. and Temsah, R.M. Sarcoplasmic reticulum and cardiac oxidative stress: an emerging target for heart disease. *Expert Opin. Ther. Targets* 5: 205-217, 2001.
5. Freedman, S.B., Isner, J.M. Therapeutic angiogenesis for ischemic cardiovascular disease. *J. Mol. Cell. Cardiol.* 33: 379-393, 2001.
6. Hao, X., Månsson-Broberg, A., Grinnemo, K.H., Siddiqui, A.J., Dellgren, G., Brodin, L.A. and Sylvén, C. Myocardial angiogenesis after plasmid or adenoviral VEGF-A(165) gene transfer in rat myocardial infarction model. *Cardiovasc. Res.* 73: 481-487, 2007.
7. Hedman, M., Hartikainen, J., Syvanne, M., Stjernvall, J., Hedman, A., Kivela, A., Vanninen, E., Mussalo, H., Kauppila, E., Simula, S., Narvanen, O., Rantala, A., Peuhkurinen, K., Nieminen, M.S., Laakso, M. and Yla-Herttuala, S. Safety and feasibility of catheter-based local intracoronary vascular endothelial growth factor gene transfer in the prevention of postangioplasty and in-stent restenosis and in the treatment of chronic myocardial ischemia: phase II results of the Kuopio Angiogenesis Trial (KAT). *Circulation* 107: 2677-2683, 2003.
8. Hoppeler, H. and Vogt, M. Muscle tissue adaptations to hypoxia. *J. Exp. Biol.* 204: 3133-3139, 2001.
9. Hsu, J.L., Huang, S.Y., Shiea, J.T., Huang,W.Y. and Chen, S.H. Beyond quantitative proteomics: signal enhancement of the a1 ion as a mass tag for peptide sequencing using dimethyl labeling. *J. Proteome. Res.* 4: 101-108, 2005.
10. Huang, S.Y., Tsai, M.L., Wu, C.J., Hsu, J.L., Ho, S.H. and Chen, S. H. Quantitation of protein phosphorylation in pregnant rat uteri using stable isotope dimethyl labeling coupled with IMAC. *Proteomics* 6: 1722-1734, 2006.
11. Jugdutt, B.I. and Sawicki, G. AT1 receptor blockade alters metabolic, functional and structural proteins after reperfused myocardial infarction: detection using proteomics. *Mol. Cell. Biochem.* 263: 179-188, 2004.
12. Kim, N., Lee, Y., Kim, H., Joo, H., Youm, J.B., Park, W.S., Warda, M., Cuong, D.V. and Han, J. Potential biomarkers for ischemic heart damage identified in mitochondrial proteins by comparative proteomics. *Proteomics* 6: 1237-1249, 2006.
13. Koransky, M.L., Robbins, R.C. and Blau, H.M. VEGF gene delivery for treatment of ischemic cardiovascular disease. *Trends Cardiovas. Med.* 12: 108-114, 2002.
14. Li, Y., Muruve, D.A., Collins, R.G., Lee, S.S. and Kubes, P. The role of selectins and integrins in adenovirus vector-induced neutrophil recruitment to the liver. *Eur. J. Immunol.* 32: 3443-3452, 2002.
15. Lohan, J. and Ohlendieck, K. Drastic reduction in the luminal Ca^{2+} -binding proteins calsequestrin and sarcalumenin in dystrophin-deficient cardiac muscle. *Biochim. Biophys. Acta* 1689: 252-258, 2004.
16. Lopez, A.D. and Murray, C.C. The global burden of disease, 1990-2020. *Nature Med.* 4: 1241-1243, 1998.
17. Losordo, D.W. and Dimmeler, S. Therapeutic angiogenesis and vasculogenesis for ischemic disease. Part I: angiogenic cytokines. *Circulation* 109: 2487-2491, 2004.
18. Losordo, D.W., Vale, P.R., Symes, J.F., Dunnington, C.H., Esakof, D.D., Maysky, M., Ashare, A.B., Lathi, K. and Isner, J.M. Gene therapy for myocardial angiogenesis: initial clinical results with direct myocardial injection of phVEGF165 as sole therapy for myocardial ischemia. *Circulation* 98: 2800-2804, 1998.
19. Lutter, G., Attmann, T., Heilmann, C., von Samson, P., von Specht, B. and Beyersdorf, F. The combined use of transmyocardial laser revascularization (TMLR) and fibroblastic growth factor (FGF-2) enhances perfusion and regional contractility in chronically ischemic porcine hearts. *Eur. J. Cardiothorac. Surg.* 22: 753-761, 2002.
20. Michiels, C. Physiological and pathological responses to hypoxia. *Am. J. Pathol.* 164: 1875-1882, 2004.
21. Remondino, A., Rosenblatt-Velin, N., Montessuit, C., Tardy, I., Papageorgiou, I., Dorsaz, P.A., Jorge-Costa, M. and Lerch, R. Altered expression of proteins of metabolic regulation during remodeling of the left ventricle after myocardial infarction. *J. Mol. Cell. Cardiol.* 32: 2025-2034, 2000.
22. Scaldaferri, F., Vetrano, S., Sans, M., Arena, V., Straface, G., Stigliano, E., Repici, A., Sturm, A., Malesci, A., Panes, J., Yla-Herttuala, S., Fiocchi, C. and Danese, S. VEGF-A links angiogenesis and inflammation in inflammatory bowel disease pathogenesis. *Gastroenterology* 136: 585-595, 2009.
23. Schirle, M., Heurtier, M.A. and Kuster, B. Profiling core proteomes of human cell lines by one-dimensional PAGE and liquid chromatography-tandem mass spectrometry. *Mol. Cell. Proteom.* 2: 1297-1305, 2003.
24. Schwarz, E.R., Speakman, M.T., Patterson, M., Hale, S.S., Isner, J. M., Kedes, L.H. and Kloner, R.A. Evaluation of the effects of intramyocardial injection of DNA expressing vascular endothelial growth factor (VEGF) in a myocardial infarction model in the rat—angiogenesis and angioma formation. *J. Am. Coll. Cardiol.* 35: 1323-1330, 2000.
25. Stanley, W.C., Recchia, F.A. and Lopaschuk, G.D. Myocardial substrate metabolism in the normal and failing heart. *Physiol. Rev.* 85: 1093-1129, 2005.
26. Stanton, L.W., Garrard, L.J., Garrick, B.L., Lam, G.A., Kapoun, A. M., Zheng, Qiang., Protter, A.A., Schreiner, G.F. and White, R.T. Altered patterns of gene expression in response to myocardial infarction. *Cir. Res.* 86: 939-945, 2000.
27. Tanaka, E., Hattan, N., Ando, K., Ueno, H., Sugio, Y., Mohammed, M.U., Voltchikhina, S.A. and Mori, H. Amelioration of microvascular myocardial ischemia by gene transfer of vascular endothelial growth factor in rabbits. *J. Thorac. Cardiovas. Surg.* 120: 720-728, 2000.
28. Taylor, S.W., Fahy, E., Zhang, B., Glenn, G.M., Warnock, D.E., Wiley, S., Murphy, A.N., Gaucher, S.P., Capaldi, R.A., Gibson, B.W. and Ghosh, S.S. Characterization of the human heart mitochondrial proteome. *Nature Biotech.* 21: 281-286, 2003.
29. Vajanto, I., Rissanen, T.T., Rutanen, J., Hiltunen, M.O., Tuomisto, T.T., Arve, K., Närvänen, O., Manninen, H., Räsänen, H., Hippeläinen, M., Alhava, E. and Ylä-Herttuala, S. Evaluation of angiogenesis and side effects in ischemic rabbit hindlimbs after intramuscular injection of adenoviral vectors encoding VEGF and LacZ. *J. Gene Med.* 4: 371-380, 2002.
30. Vale, P.R., Losordo, D.W., Milliken, C.E., Maysky, M., Esakof,

D. D., Symes, J.F. and Isner, J.M. Left ventricular electromechanical mapping to assess efficacy of phVEGF(165) gene transfer for therapeutic angiogenesis in chronic myocardial ischemia. *Circulation* 102: 965-974, 2000.

31. Zaiss, A.K., Liu, Q., Bowen, G.P., Wong, N.C., Bartlett, J.S. and Muruve, D.A. Differential activation of innate immune responses by adenovirus and adeno-associated virus vectors. *J. Virol*. 76: 4580-4590, 2002.
32. Zittermann, S.I. and Issekutz, A.C. Endothelial growth factors VEGF and bFGF differentially enhance monocyte and neutrophil recruitment to inflammation. *J. Leukoc. Biol*. 80: 247-257, 2006.